

Title: Glucose pathways adaptation supports acquisition of activated microglia phenotype

Authors: Gimeno-Bayón J, López-López A, Rodríguez MJ, Mahy N

Authors affiliation:

Unitat de Bioquímica i Biologia Molecular, Facultat de Medicina, Institut d'Investigacions Biomèdiques August Pi i Sunyer (IDIBAPS), Universitat de Barcelona, Barcelona, CIBERNED, Spain

Short running title: Activated microglia metabolic reprogramming

Author for correspondence: J. Gimeno-Bayón

Unitat de Bioquímica i Biologia Molecular

Facultat de Medicina, UB

c/ Casanova 143

E-08036 Barcelona, SPAIN

Phone: +34 93 402 0586

FAX: + 34 93 403 5882

e-mail: meno2020@gmail.com

Grant Information: This research was supported by grants IPT- 2011-1091-900000 and IPT-2012-0614-010000 from the Ministerio de Economía, and by the 2009SGR1380 grant from the Generalitat de Catalunya. A.L.L. holds a fellowship from the Institut d'Investigacions Biomèdiques August Pi i Sunyer (IDIBAPS).

ABSTRACT

With its capacity to survey the environment and phagocyte debris, microglia assume a diversity of phenotypes to specifically respond through neurotrophic and toxic effects. While these roles are well accepted, the underlying energetic mechanisms associated with microglia activation remain largely unclear. In this paper, microglia metabolic adaptation to ATP, NADPH, H⁺ and ROS production was investigated. To this end, in vitro studies were performed in BV-2 cells before and after activation with LPS+IFN γ . NO was measured as a marker of cell activation. Our results show that microglia activation triggers a metabolic reprogramming based on an increased glucose uptake and a strengthening of anaerobic glycolysis, as well as of the pentose pathway oxidative branch, while retaining the mitochondrial activity. Based on this energy commitment, microglia defense capacity increases rapidly as well as ribose-5-phosphate and nucleic acid formation for gene transcription, essential to ensure the new acquired functions demanded by CNS signaling. In discussion, we review the role of NO in this microglia energy commitment that positions cytotoxic microglia within the energetics of the astrocyte-neuron lactate shuttle.

Key words:

Glutamate-glutamine cycle, glycolysis, lactate, Nitric Oxide, Pentose phosphate pathway

Introduction

In the central nervous system (CNS), quiescent microglia constitutes the first line of defense (Falsig et al. 2008) that reacts to acute damage or infectious agents. In a dynamic equilibrium between the lesion progression and the environment, microglia adopts a diversity of phenotypes ranging from the pro-inflammatory M1 to the neurotrophic M2 (Luo and Chen 2012). So, in response to a diversity of signals, the microglia transition to an activated state implies migration to the lesioned area, induction of phagocytosis, massive changes in gene expression, and reorganization of the cell phenotype to directly modify neuronal survival. Thus, in the same environment activated microglia interferes the responses of supporting cells through release of a diversity of factors (Kettenmann et al. 2011).

Microglia express a broad set of genes encoding proteins that include but are not limited to cytokines, chemokines, neurotrophins, neurotoxic factors, and proteases. Depending on the intensity of damage and the time post-injury, a crosstalk with neurons and astrocytes induces adaptation of the microglia phenotype to favor debris clearance, necrosis, tissue repair or regeneration (De Yebra et al. 2006). For example, with a proper timing and mode of activation, microglia work as efficient antigen-presenting cells that stimulate T cells and affect the milieu balance between neurotrophism and cytotoxicity.

Reactive microglia mediate this diversity of processes in coordination with reactive astrocytes, and both cell types depend on glucose metabolism for feeding their activities. After glucose uptake, Hexokinase (HK; E.C. 2.7.1.1) mediates glucose phosphorylation, yielding glucose-6-phosphate (G6P), a

common precursor of glycolysis for energy and lactate production, and of the pentose-phosphate pathway (PPP). In microglia, the PPP not only renders ribose-5-phosphate for nucleic acid synthesis, but also NADPH+H⁺ redox equivalents through its oxidative branch, to be transformed at the external cytoplasm membrane by NADPH oxidase (E.C. 1.6.3.1) in superoxide ions for defense and oxidative stress (Wu et al. 2006; Yang et al. 2007). The rate-limiting step in glycolysis activity is catalyzed by 6-phosphofructokinase (PFK1; E.C. 2.7.1.11), and in PPP activity by glucose-6-phosphate dehydrogenase (G6PD; E.C. 1.1.1.49). The interconnected reactions between these two pathways facilitate a direct and rapid metabolic modulation that covers at each moment the cell demand in these diverse end products.

Presently, the adaptation of glucose pathways to feed microglia diversity of phenotypes remains unknown, and we hypothesized that it might in part mimic the adaptation described in astrocytes. In astrocytes, nitric oxide (NO) formation triggers a very rapid PFK1 activation that potentiates anaerobic glycolysis versus the oxidative phosphorylation (OXPHOS). This metabolic transition preserves astrocytes from ATP depletion and maintains their mitochondrial membrane potential (Almeida et al. 2004b).

To this end, *in vitro* metabolic studies were performed in BV-2 microglia, a suitable alternative model of primary culture (Henn et al. 2009), before and after activation with LPS+ IFN γ , and NO production measured in each condition (Blasi et al. 1990). Here we provide evidences that, associated with NO formation, activation of microglia triggers a metabolic reprogramming based on an increased glucose uptake and a potentiation of both the anaerobic glycolysis and the oxidative branch of PPP, while retaining a mitochondrial activity.

Essential to ensure the new functions of activated microglia, ribose-5-phosphate availability for nucleic acid synthesis and gene transcription increases rapidly as well as ATP, lactate and NADPH+H⁺. In Discussion the role of microglia lactate formation and glutamate uptake is considered positioned within the neuroenergetics of the astrocyte-neuron lactate shuttle (ANLS) (Bouzier-Sore et al. 2003; Magistretti 2006; Magistretti and Chatton 2005; Pellerin and Magistretti 2012) of a four-partite synapse, in which lactate is shuttling to neurons not only from astrocytes but also from microglia (Rodríguez MJ 2013).

Materials and methods

Materials

Cell line of murine BV-2 microglia was purchased from Cell Bank (Interlab Cell Line Collection, ICLC, Geneva, Italy). RPMI medium supplemented with L-glutamine was purchased from GIBCO (Oklahoma, USA). Fetal Bovine Serum (FBS), was from VWR Scientific (San Francisco, USA). Culture plates and flasks were purchased from Nunc (Roskilde, Denmark). Lipopolysaccharide (LPS) from *Escherichia coli* 0111:B4 and interferon-gamma (IFN γ) and all metabolites and enzyme reagents were purchased from Sigma (St. Louis, USA).

BV-2 cell culture

BV-2 cells were cultured in RPMI 1640 medium with L-glutamine and supplemented with 10% (v/v) heat-inactivated FBS, 100 U/ml penicillin and 100

$\mu\text{g/ml}$ streptomycin. Cells were grown in a humidifier cell incubator containing 5% CO_2 at 37 °C. Before activation, cells were cultured at a density of 5×10^4 cells/ml for 24 h and flasks were divided into 3 groups: a) One group with no further manipulation, called Control, b) the LPS+ IFN γ group, in which BV-2 cells were activated with LPS+ IFN γ (0.1 $\mu\text{g/ml}$ and 0.5 ng/ml respectively) for 24 hours, and c) the IL-4 group, in which BV-2 cells were stimulated with IL-4 (0.5 $\mu\text{g/ml}$) for 24 hours.

Inhibition of NO synthesis in LPS+IFN γ stimulated BV-2 cells

In order to inhibit NO formation, BV-2 cells activated with LPS+IFN γ were incubated with 2.5 mM N ω -nitro-L-arginine (NLA), a potent inhibitor of nitric oxide synthase (NOS) (Molnár and Hertelendy 1992).

Quantification of NO and TNF α production by BV-2 cells

NO production was assessed in culture supernatants by the Griess reaction, a colorimetric assay that detects nitrite (NO_2^-) as a stable reaction product of NO with molecular oxygen (Green et al., 1982). Briefly, 50 μl of each sample were incubated with 25 μl of Griess reagent A (1% sulfanilamide, 5% phosphoric acid) and 25 μl of Griess reagent B (0.1% N-1-naphthylenediamine) for 5 min. Sample optical density was measured at 540 nm with a microplate reader (Sunrise-Basic Reader, TECAN). The nitrite concentration was determined from a sodium nitrite standard curve. TNF α released in the cell culture supernatant was determined by an ELISA murine TNF α kit (PeproTech; London, UK) following the manufacturer's guidelines.

Real-time RT-PCR

Total RNA from microglial cells was isolated using the NucleoSpin® RNA/Protein kit (Qiagen Inc., Hilden, Germany) according to the manufacturer's instructions. Then 2 µg of first-strand cDNA was synthesized with random primers using the First Strand cDNA Synthesis kit. The RT reaction was performed at 42°C for 60 minutes and then at 70°C for 5 minutes. Real-time PCR was conducted using SensiFAST® SYBR No-ROX One-Step mix and Applied Biosystems (Foster, CA) Stem One Plus® Real Time PCR Systems according to manufacturer's instructions. The PCR program was: 2 minutes at 95°C for denaturation, subsequently 45 cycles of 15 seconds at 95°C for amplification, and 1 minute at 60°C for final extension.. The level of mRNA expression was determined with a standard curve and normalized to the mRNA level of B2m. The PCR primer of B2m endogenous control, glucose transporters (GLUT) -1, -2 -3, -4, and -5, and glucokinase (GK) target genes were purchased from RealTimePrimers (Elkins Park PA, USA) The $\Delta\Delta C_T$ method was used to analyze the data as described by Bookout et al. (2006). Primer sequences for target gene and endogenous controls are presented in Table 1.

Glucose consumption and Lactate production

Culture medium was collected from control and LPS+IFN γ activated BV-2 cells at time 0 and 24 hours. Then glucose and lactate levels were determined with an ADVIA® 2400 Clinical Chemistry System (Siemens Healthcare Diagnostics, Tarrytown, USA) that uses the glucose oxidase method described by Barham and Trinder (Barham and Trinder 1972) and the method of Shimojo (Shimojo et

al. 1989) for lactate measurement. For statistical analysis of lactate release, a normal distribution of data was assumed (Voisin et al. 2010).

Lysate preparation and enzyme activity determination

Cells were grown to confluence, transferred to a 15 ml Falcom® tube (BD Biosciences, California, USA), centrifuged at 1000x g at RT for 10 min. Pelleted cells were washed in 10 ml PBS 10 mM PH=7.4, counted in a Neubauer counting chamber and centrifuged again. The pellet was suspended in enough amount of ice-cold lysis buffer (50 mM Tris-HCl, 4 mM EDTA, 50 mM FK, 0,1% (v/v) Triton X-100, PH=7) to have 10^7 cells/ml, transferred to a 1.5 ml centrifuge tube and homogenized (Potter's Homogeneizer) at 11000 min^{-1} . Then, the cell lysate was centrifuged at 14000 g for 15 min at 4°C. The supernatant fraction was transferred to a centrifuge tube and stored at 4°C until the enzymatic assay was performed.

The enzyme activities of HK, PFK1, G6PDH and lactate dehydrogenase (LDH; E.C. 1.1.1.27) were estimated spectrophotometrically in BV-2 lysate supernatants. The assays were performed at 30°C in 1 ml final volume incubation buffer added with 100 µl cell supernatant in a Beckman Coulter (Brea, USA) recording spectrophotometer. Then concentration of NADH or NADPH was monitored by measuring absorbance at 340 nm. One unit of enzyme activity (U) is defined as µmol/min, and specific activity is expressed as U/n°cells.

HK activity was assayed by measuring the rate of reduction of NADP^+ by

glucose 6-phosphate dehydrogenase (Bergmeyer 1983). The assay medium contained Tris-HCl 50 mM, MgSO₄ 80 mM, EDTA 20 mM, KCl 1.5 mM, mercaptoethanol 2mM, NADP⁺ 3 mM, ATP 2.5 mM, Triethanolamine 200 mM, Glucose 1 mM.

PFK1 activity was measured by measuring changes in the absorbance of NADH in a coupled enzyme assay (Beutler 1975). The assay buffer consisted of Tris-HCl 50 mM, pH 7.4, MgCl₂ 100 mM, EDTA 5 mM, aldolase (mouse muscle, 0.04 U/ml), triose phosphate isomerase (mouse muscle, 2.4 U/ml), GAPDH (mouse muscle, 0.32 UI/ml) and 1mM of fructose 6-phosphate and ATP.

Lactate dehydrogenase activity was measured using the method previously described by Hakala (Hakala et al. 1956). The assay buffer consisted of Tris-HCl 50mM PH=7.5, NADH 2 mM and pyruvate 20mM.

G6PDH activity was assayed as described by Bishop (Bishop 1966). The assay medium contained 380 mM glycine, 304 mM hydrazine, 83 mM Lactate and 2,6 mM NAD disodium salt.

Confocal imaging of mitochondrial membrane potential

Mitochondrial membrane potential ($\Delta\Psi_m$) was measured by confocal imaging of BV-2 cells loaded with the fluorescent probe tetramethylrhodamine ethyl ester (TMRE) (Molecular Probes, Eugene Oregon), as previously described (Baczkó et al. 2004). In brief, cells were first incubated in 6 well-plates for 30 min in medium containing TMRE (50 nM) and then washed with fresh medium.

Afterwards, cells were incubated in the presence of 50 nM TMRE during the imaging process. Cell fluorescence was acquired by sequential scanning at the 510 nm emission wavelength. Cell average pixel intensity was obtained as an average of measurements done in 4 fields of each one of 3 culture wells.

Confocal images were obtained using Zeiss Observer.Z1® microscope coupled to a Retiga EXi Fast 1394® camera, objective LD 20X/0.4 DICII (resolution 0.83 μm).

Software and Data analysis

Statistical studies and graphics were performed with Statgraphics® (STSC Inc., Rockville, USA) and Graphpad Prism® (GraphPad Software Inc., La Jolla, USA). For each parameter, Kurtosis and Skewness moments were calculated to test the normal distribution of data. One-way ANOVA test was used to analyse differences between the groups. In all cases $p < 0.05$ was considered statistically significant.

Image acquisition was performed using Fluo4® software (Exploranova, Bordeaux, France). Figure 5 was produced using Servier Medical Art archive (Les laboratoires servier, Suresnes, France)

Results

BV-2 cell activation increases glucose uptake and its phosphorylation

BV-2 cell activation was monitored by estimation of NO and TNF α release 24h

after activation with LPS+IFN γ . At this time, LPS+IFN γ increased 6 fold NO production (from 4.89 ± 0.85 to 29.62 ± 1.96 $p < 0.0001$) and TNF α 3.5-fold (from 534.88 ± 113.94 to 1948.58 ± 333.32 $p < 0.0001$) when compared with controls.

BV-2 glucose consumption was compared between control and LPS+IFN γ activated cells. In both situations, glucose was measured in the culture medium at time 0 and 24h, and results were referred to the BV-2 cell number. After activation, glucose consumption increased significantly in a fold change of 1.37 (Figure 1A, 2D).

An increased energy demand requires greater microglia usage of glucose, and in other cells this is facilitated by the increased activity of Hexokinase to retain glucose within the cell, and also by the increased expression of GLUT. To estimate the effect of cell activation on the glucose uptake and consumption by microglia we determined the HK specific activity and the expression of GK and the five main species of GLUT. Relative to control, LPS+IFN γ promoted a significant 1.9-fold increase of HK specific activity in the soluble fraction of cell lysate (Figure 1B, 2D). BV-2 glucokinase expression was analyzed by RT-qPCR. mRNA of this enzyme was amplified from total RNA isolated from control BV-2 cells, and no change was found after LPS+IFN γ activation (data not shown).

To identify which of the five members of the GLUT family are expressed in microglia, mRNA of GLUT-1 to -5 was analyzed in control cells by RT-qPCR. GLUT-1 expression resulted largely predominant (91% of total), far from GLUT-

4 the second in abundance (8,2% of total) (Figure 1C). The very low expression of GLUT-2, GLUT-3 and GLUT-5 (< 0,2% of total) was considered negligible (Figure 1C). 24h after LPS+IFN γ activation, both GLUT-1 and GLUT-4 expression resulted similarly increased, but this increase was significant for GLUT-4 ($p=0.034$) and not for GLUT1 ($p=0,057$). GLUT-2, GLUT-3 and GLUT-5 levels remained negligible (Figure 1C).

BV-2 cell activation induces a switch of glucose metabolism to anaerobic glycolysis and pentose phosphate pathway.

The increased glucose uptake and its phosphorylation measured in activated BV-2 cells may indicate an enhancement of anaerobic glycolysis, supported by the increased activity of PFK1, the key regulatory enzyme of the glycolytic rate. This enhancement is sometimes associated with an increased ROS production at the plasma membrane facilitated by the increased activity of G6PDH, the regulatory enzyme of the PPP.

Consistent with this possibility, G6PDH specific activity was determined in the soluble fraction of cell lysate, together with PFK1 and LDH specific activities and lactate extracellular concentration. Relative to control, LPS+IFN γ activation promoted at 24h a significant increase of G6PDH specific activity in a 1.95 fold change ($p=0.004$, Figure 2A,D). PFK1 specific activity resulted also significantly increased in a 1.14 fold change ($p=0.0014$, Figure 2B,D), and the same occurred with LDH activity, increased in a fold change of 1.4 ($p<0.0001$, Figure 2C,D).

Compared to control, lactate production was doubled in the activated cells, as evidenced at 24h by its 2.02-fold increased concentration in the culture medium ($p=0.019$). Besides the increased glucose uptake of the activated cells, the lactate level represents an increased and massive transformation of G6P into lactate, supported by a glucose/lactate ratio from 1.266 in controls to 1.874 in activated cells.

This massive lactate production could be attributed to a reduced mitochondrial activity and a switch to anaerobic glycolysis of the activated cells. This was assessed through a time-lapse confocal imaging of the inner membrane potential ($\Delta\Psi_m$) at 24h in control and activated cells with the mitochondrial membrane potential sensitive dye TMRE (3A). In both situations, the frequency distribution of mitochondria fluorescence followed a normal distribution and was similar in their absolute value and relative frequency distribution (Figure 3B). The lack of $\Delta\Psi_m$ difference herein found indicates that the activated cells maintain their electron transport chain usage besides their anaerobic glycolysis switch and their increased PPP.

NO formation participates of the activated BV-2 cells glycolytic activation

Involvement of NO in the metabolic reprogramming of LPS+IFN γ activated BV-2 cells was studied after 2'5 mM N ω -nitro-l-arginine inhibition of iNOS for 24h. Glucose and lactate were measured in the culture medium at time 0 and 24h, and results referred to the BV-2 cell number. iNOS inhibition resulted in a decreased of both glucose consumption (fold change of 0.82, $p=0.02$) and lactate release (fold change of 0.63, $p<0.001$) (Figure 4A, B), back to control

values. No significant change in G6PDH was found (Figure 4C), indicating that its activation is independent from NO.

BV-2 cells adoption of a phagocytic phenotype activates a new metabolic reprogramming

To determine whether our results also apply to the adoption of a phagocytic phenotype, BV-2 cells were stimulated with IL-4 (0.5 $\mu\text{g/ml}$) for 24h. Glucose and Lactate were both measured in the culture medium at time 0 and 24h, and G6PDH activity in the homogenate as usually. With regard to control, glucose consumption was 30% reduced ($p < 0.001$) and lactate production 43% ($p < 0.006$), whereas G6PDH activity resulted unchanged. In these conditions, the maintenance of the PPP ensures NADPH+H⁺ redox equivalents to be transformed in superoxide ions for phagocytosis as G6DPH strongly increases its activity with higher NADP⁺ level. The new biomolecules delivered by phagocytosis directly available to the BV-2 cells would reduce at least in part the need of anabolic reactions and thus the cell energy demand. This possibility requires further experiments to be validated.

Discussion

BV- 2 cells were used to investigate the microglia adaptation to an excitotoxic phenotype. This cell line is considered a suitable alternative model of primary culture or of many animal studies (Henn et al. 2009) (Stansley et al. 2012). For example, 90% of the genes induced in BV-2 by LPS activation are also found in primary microglia, including the Nitric Oxide synthase (iNOS) gene. 24h after

incubation with LPS+IFN γ , BV-2 cells increased NO and TNF α production that is related with an enhancement of cell inflammatory activity (Ortega et al. 2013). In these conditions, the main finding of this study is the coordinated response of the glucose pathways necessary to cover the cell demand and enable the microglia response to activation. This metabolic reprogramming is different with microglia adoption of a phagocytic phenotype as the delivery of new biomolecules may reduce the cell energy demand. In astrocytes LPS stimulation induced NO production leading to an increased glucose consumption and lactate release (Bolaños et al. 1994) and an increased PPP activity to prevent glutathione depletion and increase astrocyte resistance to NO mediated cellular damage (García-Nogales et al. 1999). After exposure to peroxynitrite, the maintenance of astrocyte mitochondrial activity and its reduction in neurons also demonstrates the astrocytic resistance capacity to NO damage (Bolaños et al. 1995). The direct NO participation in the microglia metabolic reprogramming shown by our data reinforces the similarity with the astrocyte metabolic adaptation to excitotoxicity. As such, the increased HK activity and increased GLUT1 and GLUT4 expression ensure enough glucose availability to the cell. GLUT1 expression in control microglia was much higher than GLUT4, with similar changes 24h after activation. Because of that, these two transporters can be considered constitutive of microglia.

GLUT1 is a high-affinity glucose transporter, which expression in tumor cells is stimulated under hypoxic conditions. And this adaptation also includes enhancement of the glycolysis rate to support the increased energy demand of the proliferative cells (Bashan et al. 1992; Haber et al. 1998). The HK and

GLUT1 increases herein found would then reflect the microglia adaptation to an enhanced glycolytic demand with a high lactate production, and high metabolic rate. GLUT4 expression is modulated in brain and pancreas by ATP dependent potassium (K_{ATP}) channels whose activity depends on glucokinase (Choeiri et al. 2006). In agreement with previous brain studies (Alvarez et al. 2002) the low glucokinase K_m that renders the enzyme unable to detect glucose concentration increase may explain the unchanged glucokinase expression in activated microglia. The increased K_{ATP} channel expression described in activated microglia (Ortega et al. 2012; Ramonet et al. 2004b) may then participate in the GLUT4 expression increase. If true, the similar changes of GLUT1 and GLUT4 shown by our results suggest a coordinated microglia control of their expression that may depend, at least in part, on K_{ATP} channel activity. As observed in taste cells (Yee et al. 2011), this would represent a fine coordination between activation of microglia and increased glucose availability.

Microglia metabolic reprogramming led to a potentiation of anaerobic glycolysis reflected by the increased PFK1 and LDH activities and a massive lactate formation. In astrocytes increased NO stimulates PFK1 activity through allosteric activation with fructose-2,6-bisphosphate (Fru-2,6-P₂) produced by 6-phosphofructo-2-kinase/fructose-2,6-bisphosphatase. Moreover, NO inhibition of cytochrome c oxidase switches the glycolytic rate on, with pyruvate conversion into lactate recovering NAD⁺ in the cytosol for glycolysis feed-back (Almeida et al. 2004a). The supply of glucose-derived lactate by activated microglia would support active neurons, whose elevated energy demand relies mostly on mitochondrial ATP production. Thus, with the astrocytes and

microglia adapted to a major glucose anaerobic oxidation, lactate represents the major neuronal energy source in damaged CNS (Fig 5).

The NO-mediated down-regulation of mitochondrial energy production observed in neurons and initially in astrocytes (Bolaños et al. 1994), but afterwards considered to be unaffected by the same authors, with similar activities of the enzymatic complexes of the Krebs cycle (Bolaños et al. 1995) was not truly observed in microglia. The similar $\Delta\Psi_m$ of control and activated BV-2 cells might reflect the ATP synthase reversed reaction fed by ATP from glycolysis and others (Almeida et al. 2001 PNAS), or could indicate an active electron transport chain energy production. In microglia of damaged brain tissue, the higher number of mitochondria labeled with [H^3]PK11195 (Bernal et al. 2009; De Yebra et al. 2006) and their higher K_{ATP} channels expression (Rodríguez MJ 2013; Virgili et al. 2011) argue in favor of a significant mitochondrial production of energy to help ensuring sufficient bioenergetics to execute the new transcription programs derived from excitotoxic activation. If true, feeding of the Krebs cycle to maintain mitochondria activity cannot rely on pyruvate because of its transformation into lactate, but on 2-oxoglutarate formation from glutamate and glutamine deamination that increases progressively from apoptotic to necrotic damage (Ramonet et al. 2004a).

Upon activation, microglia express the two glutamate transporters EAAT-1 and -2 for glutamate and glutamine synaptic extrusion as well as glutamine synthase (Gras et al. 2006). Thus, in excitotoxicity, the fast microglial uptake of glutamate and glutamine, coordinated with the astrocyte glutamate removal, promotes a quick deactivation of the increased synaptic glutamate signal. In astrocytes, the

early work by Pellerin et al (1994) describes the glutamate-induced glycolysis to facilitate lactate to neurons during physiological activation, and hypothesized for the first time the ANLS. With excitotoxicity, microglia glutamate uptake would induce a similar stimulatory effect to provide further lactate to neurons, and also renders abundant 2-oxoglutarate to ensure the Krebs cycle activity.

In microglia glutamate deamination renders 2-oxoglutarate and ammonium that, combined with CO₂ released from the Krebs cycle, forms carbamic acid, a precursor of the pyrimidine bases necessary for nucleic acid synthesis and the increased gene expression. As in astrocytes (Gradinaru et al. 2012), carbamic acid direct clearance and elimination as a stable complex with glucuronides is also possible through a detoxification process (Hipkiss 2010; Schafer et al. 2013).

In necrotic brain tissue a net glutamine output of the Glutamate/Glutamine cycle caused by a reduced neuronal glutaminase activity (Ramonet et al. 2004a) increases the microglial formation of 2-oxoglutarate and ammonium and the generation of superoxide ions. After reaction with NO, superoxide ions form the highly reactive peroxynitrite products, associated with a cytotoxic microglia phenotype, and a progressive microglia dysfunction. (Svoboda and Kerschbaum 2009). If true, microglia ammonium concentration would represent one of the contextual factors that influence the microglial net effects on neuronal survival (Luo and Chen 2012) (See Fig. 5).

The PPP oxidative branch was also increased in activated microglia, as shown by the increased G6PDH activity that supports G6P oxidation and NADPH formation. In neurons NO facilitates a fine-tuning of G6P destination to glycolysis or PPP that potentiates glutathione reduction against oxidative

damage. Our data indicate that NO is also directly involved in the metabolic reprogramming of microglia, together with a significant contribution of the phagosomal NADPH-oxidase to ROS generation and oxidative stress damage from G6P (Miller et al. 2007; Wu et al. 2006). Furthermore, the juxtaposition of phagosomes and mitochondria recently proposed in microglia (Rodríguez MJ 2013) should potentiate mitochondrial ROS formation and energy production (Dikalov et al. 2012; Murphy 2009) (See Fig. 5).

In conclusion, NO appears to play a key role in the adaptation of activated microglia to the energy commitment necessary to ensure its adoption of a neurotrophic/cytotoxic phenotype. In these conditions, the coordinated response of the four-partite synapse, in which lactate is shuttling to neurons not only from astrocytes but also from microglia, has also to include the rapid glutamate removal by astrocytes and microglia. Thus, under brain damage, a new player should be included in the ANLS initially proposed by Pelerin et al. (1994), transforming it into a microglia-astrocyte-neuron lactate shuttle. Further studies are needed to determine how reduction of glutaminase activity following neuronal damage and the consequent increased ammonium output influence the microglia response of increased oxidative damage.

Acknowledgements

We thank Ivan Cester and Dra. Martínez-Moreno for technical help and Laura Gómez for performing the G6PDH activity determinations. Authors disclose any potential sources of conflict of interest.

References

- Almeida A, Moncada S, Bolaños JP. 2004a. Nitric oxide switches on glycolysis through the AMP protein kinase and 6-phosphofructo-2-kinase pathway. *NatCell Biol* 6(1):45-51.
- Almeida A, Moncada S, Bolaños JP. 2004b. Nitric oxide switches on glycolysis through the AMP protein kinase and 6-phosphofructo-2-kinase pathway. *Nat Cell Biol* 6(1):45-51.
- Alvarez E, Roncero I, Chowen JA, Vázquez P, Blázquez E. 2002. Evidence that glucokinase regulatory protein is expressed and interacts with glucokinase in rat brain. *J Neurochem* 80:45-53.
- Baczkó I, Giles WR, Light PE. 2004. Pharmacological activation of plasma-membrane KATP channels reduces reoxygenation-induced Ca(2+) overload in cardiac myocytes via modulation of the diastolic membrane potential. *British Journal of Pharmacology* 141(6):1059-1067.
- Barham D, Trinder P. 1972. An improved colour reagent for the determination of blood glucose by the oxidase system. *Analyst* 97(151):142-145.
- Bashan N, Burdett E, Hundal HS, Klip A. 1992. Regulation of glucose transport and GLUT1 glucose transporter expression by O₂ in muscle cells in culture. *Am J Physiol* 262(3 Pt 1):C682-690.
- Bergmeyer HU, Grassl, M., and Walter, H.E. 1983. *Methods of Enzymatic Analysis*. Deerfield Beach, FL: Bergmeyer, H.U.
- Bernal F, Petegnief V, Rodríguez MJ, Ursu G, Pugliese M, Mahy N. 2009. Nimodipine inhibits TMB-8 potentiation of AMPA-induced hippocampal neurodegeneration. *J Neurosci Res*. p 1240-1249.
- Beutler E. 1975. *Red Cell Metabolism. A Manual of Biochemical Methods*. Biochemical Methods (ed 2) Orlando, Fla, Grune & Stratton 2 Edition.
- Bishop C. 1966. Assay of glucose-6-phosphate dehydrogenase (E.C. 1.1.1.49) and 6-phosphogluconate dehydrogenase (E.C. 1.1.1.43) in red cells. *J Lab Clin Med* 68(1):149-155.

- Blasi E, Barluzzi R, Bocchini V, Mazzolla R, Bistoni F. 1990. Immortalization of murine microglial cells by a v-raf/v-myc carrying retrovirus. *J Neuroimmunol* 27(2-3):229-237.
- Bolaños JP, Heales SJ, Land JM, Clark JB. 1995. Effect of peroxynitrite on the mitochondrial respiratory chain: differential susceptibility of neurones and astrocytes in primary culture. *J Neurochem* 64(5):1965-1972.
- Bolaños JP, Peuchen S, Heales SJ, Land JM, Clark JB. 1994. Nitric oxide-mediated inhibition of the mitochondrial respiratory chain in cultured astrocytes. *J Neurochem* 63(3):910-916.
- Bouzier-Sore A-K, Voisin P, Canioni P, Magistretti PJ, Pellerin L. 2003. Lactate Is a Preferential Oxidative Energy Substrate Over Glucose for Neurons in Culture. *J Cereb Blood Flow Metab*:1298-1306.
- Choeiri C, Staines WA, Miki T, Seino S, Renaud J-M, Teutenberg K, Messier C. 2006. Cerebral glucose transporters expression and spatial learning in the K-ATP Kir6.2(-/-) knockout mice. *Behav Brain Res* 172(2):233-239.
- De Yebra L, Malpesa Y, Ursu G, Pugliese M, LiÇvens JC, Kerkerian-Le Goff L, Mahy N. 2006. Dissociation between hippocampal neuronal loss, astroglial and microglial reactivity after pharmacologically induced reverse glutamate transport. *Neurochemistry International* 49 (7):691-697.
- Dikalov SI, Li W, Doughan AK, Blanco RR, Zafari AM. 2012. Mitochondrial reactive oxygen species and calcium uptake regulate activation of phagocytic NADPH oxidase. *Am J Physiol Regul Integr Comp Physiol* 302(10):R1134-1142.
- Falsig J, van Beek J, Hermann C, Leist M. 2008. Molecular basis for detection of invading pathogens in the brain. *J Neurosci Res* 86(7):1434-1447.
- García-Nogales P, Almeida A, Fernández E, Medina JM, Bolaños JP. 1999. Induction of glucose-6-phosphate dehydrogenase by lipopolysaccharide contributes to preventing nitric oxide-mediated glutathione depletion in cultured rat astrocytes. *J Neurochem* 72(4):1750-1758.
- Gradinaru D, Minn A-L, Artur Y, Minn A, Heydel J-M. 2012. Effect of oxidative stress on UDP-glucuronosyltransferases in rat astrocytes. *Toxicol Lett* 213(3):316-324.

- Gras G, Porcheray F, Samah B, Leone C. 2006. The glutamate-glutamine cycle as an inducible, protective face of macrophage activation. *J Leukoc Biol* 80(5):1067-1075.
- Haber RS, Rathan A, Weiser KR, Pritsker A, Itzkowitz SH, Bodian C, Slater G, Weiss A, Burstein DE. 1998. GLUT1 glucose transporter expression in colorectal carcinoma: a marker for poor prognosis. *Cancer* 83(1):34-40.
- Hakala M, Glaid AJ, Schwert GW. 1956. Lactic dehydrogenase. II. Variation of kinetic and equilibrium constants with temperature. *J Biol Chem* 221(1):191-209.
- Henn A, Lund S, Hedtjärn M, Schratzenholz A, Pörzgen P, Leist M. 2009. The suitability of BV2 cells as alternative model system for primary microglia cultures or for animal experiments examining brain inflammation. *ALTEX* 26(2):83-94.
- Hipkiss AR. 2010. Aging, Proteotoxicity, Mitochondria, Glycation, NAD and Carnosine: Possible Inter-Relationships and Resolution of the Oxygen Paradox. *Front Aging Neurosci* 2:10.
- Kettenmann H, Hanisch U-K, Noda M, Verkhratsky A. 2011. Physiology of microglia. *Physiol Rev* 91(2):461-553.
- Luo X-G, Chen S-D. 2012. The changing phenotype of microglia from homeostasis to disease. *Transl Neurodegener* 1(1):9.
- Magistretti PJ. 2006. Neuron-glia metabolic coupling and plasticity. *J Exp Biol* 209(Pt 12):2304-2311.
- Magistretti PJ, Chatton J-Y. 2005. Relationship between L-glutamate-regulated intracellular Na⁺ dynamics and ATP hydrolysis in astrocytes. *J Neural Transm* 112(1):77-85.
- Miller RL, Sun GY, Sun AY. 2007. Cytotoxicity of paraquat in microglial cells: Involvement of PKC δ - and ERK1/2-dependent NADPH oxidase. *Brain Research* 1167:129-139.
- Molnár M, Hertelendy F. 1992. N omega-nitro-L-arginine, an inhibitor of nitric oxide synthesis, increases blood pressure in rats and reverses the pregnancy-induced refractoriness to vasopressor agents. *Am J Obstet Gynecol* 166(5):1560-1567.
- Murphy MP. 2009. How mitochondria produce reactive oxygen species. *Biochem J* 417(1):1-13.

- Ortega FJ, Jolkkonen J, Mahy N, Rodríguez MJ. 2013. Glibenclamide enhances neurogenesis and improves long-term functional recovery after transient focal cerebral ischemia. *J Cereb Blood Flow Metab* 33:8.
- Pellerin L, Magistretti PJ. 2012. Sweet sixteen for ANLS. *J Cereb Blood Flow Metab* 32(7):1152-1166.
- Ramonet D, Rodriguez MJ, Fredriksson K, Bernal F, Mahy N. 2004a. In vivo neuroprotective adaptation of the glutamate/glutamine cycle to neuronal death. *Hippocampus* 14(5):586-594.
- Ramonet D, Rodriguez MJ, Pugliese M, Mahy N. 2004b. Putative glucosensing property in rat and human activated microglia. *Neurobiology of Disease* 17:1-9.
- Rodríguez MJ M-M, M, Ortega FJ, and Mahy N. 2013. Targeting microglial KATP channels to treat neurodegenerative diseases: a mitochondrial issue. *J Oxid Med Cell Long* (In press).
- Schafer DP, Lehrman EK, Stevens B. 2013. The "quad-partite" synapse: Microglia-synapse interactions in the developing and mature CNS. *Glia* 61(1):24-36.
- Shimojo N, Naka K, Nakajima C, Yoshikawa C, Okuda K, Okada K. 1989. Test-strip method for measuring lactate in whole blood. *Clin Chem* 35(9):1992-1994.
- Stansley B, Post J, Hensley K. 2012. A comparative review of cell culture systems for the study of microglial biology in Alzheimer's disease. *J Neuroinflammation* 9:115.
- Svoboda N, Kerschbaum HH. 2009. L-Glutamine-induced apoptosis in microglia is mediated by mitochondrial dysfunction. *Eur J Neurosci* 30(2):196-206.
- Virgili N, Espinosa-Parrilla JF, Mancera P, Pastén-Zamorano A, Gimeno-Bayon J, Rodríguez MJ, Mahy N, Pugliese M. 2011. Oral administration of the KATP channel opener diazoxide ameliorates disease progression in a murine model of multiple sclerosis. *J Neuroinflammation* 8:149.
- Voisin P, Bouchaud V, Merle M, Diolez P, Duffy L, Flint K, Franconi J-M, Bouzier-Sore A-K. 2010. Microglia in Close Vicinity of Glioma Cells: Correlation Between Phenotype and Metabolic Alterations. *Front Neuroenerg* 2:1-15.

- Wu D-C, Ré DB, Nagai M, Ischiropoulos H, Przedborski S. 2006. The inflammatory NADPH oxidase enzyme modulates motor neuron degeneration in amyotrophic lateral sclerosis mice. *Proc Natl Acad Sci USA* 103(32):12132-12137.
- Yang D, Elnér SG, Bian Z-M, Till GO, Petty HR, Elnér VM. 2007. Pro-inflammatory cytokines increase reactive oxygen species through mitochondria and NADPH oxidase in cultured RPE cells. *Exp Eye Res* 85(4):462-472.
- Yee KK, Sukumaran SK, Kotha R, Gilbertson TA, Margolskee RF. 2011. Glucose transporters and ATP-gated K⁺ (KATP) metabolic sensors are present in type 1 taste receptor 3 (T1r3)-expressing taste cells. *Proc Natl Acad Sci USA* 108(13):5431-5436.

Figure legends

Figure 1: 24h after LPS+INF γ activation, the BV-2 increased glucose consumption is facilitated by the coordinated increase of hexokinase activity and GLUT-1 and GLUT-4 expression. **A:** Increase of Glucose consumption (*p<0.0001 vs control) **B:** Increase of Hexokinase specific activity (*p=0.044 vs control). (Data are normalized for cell number; Glc_i = Glucose concentration at time 0, Glc_f = Glucose concentration at time 24h). **C:** Similar increase of GLUT-1 and GLUT-4 expression measured by Quantitative PCR analysis; Ratio is measured versus a housekeeping gene (HG, beta-2-microglobulin).

Figure 2: Coordinated BV-2 cell metabolic adaptation to LPS+INF γ activation. **A:** Glucose-6-phosphate deshydrogenase (G6PDH) specific activity normalized by number of cells (*p=0.004). **B:** Phosphofructokinase-1 (PFK) specific activity normalized by cell concentration (*p=0.0014) **C:** Lactate deshydrogenase (LDH) specific activity normalized by cell concentration (*p<0.0001 vs control). **D:** Lactate released by BV-2 cells (*p=0.019 vs control). **E:** BV-2 cell activation increases both Glucose uptake and its transformation to lactate. (Conc. in mg.dl⁻¹. 10⁶cell⁻¹, and enzyme activities in U. 10⁶cell⁻¹).

Figure 3: Mitochondrial membrane potential of activated and non activated microglial BV2 cells. Confocal image of control (**A**) and LPS+INF γ activated (**B**) BV-2 cells loaded with the mitochondrial membrane potential sensitive dye

TMRE (40x image). **C**: Frequency distribution of mitochondrial TMRE

fluorescence in control and LPS+INF activated BV-2 cells.

Figure 4: Effect of stimulation with IL-4 and inhibition of iNOS with NLA in BV-2 cells metabolism (Data are normalized for cell number). **(A)** Glucose consumption was 30% reduced by IL-4 (* $p < 0.001$ vs control) in control BV2 cells, and NLA reduced 18% glucose consumption when applied to activated cells (# $p = 0.02$, LPS+IFN+NLA vs LPS+IFN) **(B)** Lactate release was 44% reduced by IL-4 (* $p < 0.001$ vs control) and NLA reduced 38% this lactate production in activated cells (# $p = 0.001$, LPS+IFN+NLA vs LPS+IFN). **(C)** IL-4 and inhibition of iNOS with NLA did not modified G6PDH activity.

Figure 5. Proposed microglia-astrocyte-neuron lactate shuttle (MANLS).

After microglia activation with LPS+IFN, glucose is mostly oxidized by astrocytes and microglia and converted into lactate that is taken up by neurons for its complete oxidation. Glutamine and glutamate synaptic removal by microglia fuels the tricarboxylic acid cycle to maintain mitochondrial activity and ATP generation. Initially the resulting ammonium facilitates carbamic acid synthesis for pyrimidine formation and can also be cleared as carbamic acid glucuronides.

Dashed arrows: Type 1 represents glutamine and glutamate cycle. Type 2 represent glucose metabolism. Type 3 represent non direct metabolic connections. Type 4 ammonia uptake. Glc: glucose, Glu: glutamate, Gln: glutamine, Pyr: pyruvate, Lac: lactate, G6P: glucose-6-phosphate, G3P: glucose-3-phosphate, F6P: fructose-6-phosphate, Ri5P: ribulose-5-phosphate, R5P: ribose-5-phosphate, KG: alpha ketoglutarate. NADPH: Nicotinamide adenine

dinucleotide phosphate, NTs: Nucleotides, ROS: reactive oxygen species. TCA: tricarboxylic acid cycle, CbA: carbamic acid, CbA-GC: glucuronic acid synthesis from carbamic acid. NH_4^+ : Ammonium, CO_2 : carbon dioxide

Title: Glucose pathways adaptation supports acquisition of activated microglia phenotype

Authors: Gimeno-Bayón J, López-López A, Rodríguez MJ, Mahy N

Authors affiliation:

Unitat de Bioquímica i Biologia Molecular, Facultat de Medicina, Institut d'Investigacions Biomèdiques August Pi i Sunyer (IDIBAPS), Universitat de Barcelona, Barcelona, CIBERNED, Spain

Short running title: Activated microglia metabolic reprogramming

Author for correspondence: J. Gimeno-Bayón

Unitat de Bioquímica i Biologia Molecular

Facultat de Medicina, UB

c/ Casanova 143

E-08036 Barcelona, SPAIN

Phone: +34 93 402 0586

FAX: + 34 93 403 5882

e-mail: meno2020@gmail.com

Grant Information: This research was supported by grants IPT- 2011-1091-900000 and IPT-2012-0614-010000 from the Ministerio de Economía, and by the 2009SGR1380 grant from the Generalitat de Catalunya. A.L.L. holds a fellowship from the Institut d'Investigacions Biomèdiques August Pi i Sunyer (IDIBAPS).

ABSTRACT

With its capacity to survey the environment and phagocyte debris, microglia assume a diversity of phenotypes to specifically respond through neurotrophic and toxic effects. While these roles are well accepted, the underlying energetic mechanisms associated with microglia activation remain largely unclear. In this paper, microglia metabolic adaptation to ATP, NADPH, H⁺ and ROS production was investigated. To this end, in vitro studies were performed in BV-2 cells before and after activation with LPS+IFN γ . NO was measured as a marker of cell activation. Our results show that microglia activation triggers a metabolic reprogramming based on an increased glucose uptake and a strengthening of anaerobic glycolysis, as well as of the pentose pathway oxidative branch, while retaining the mitochondrial activity. Based on this energy commitment, microglia defense capacity increases rapidly as well as ribose-5-phosphate and nucleic acid formation for gene transcription, essential to ensure the new acquired functions demanded by CNS signaling. In discussion, we review the role of NO in this microglia energy commitment that positions cytotoxic microglia within the energetics of the astrocyte-neuron lactate shuttle.

Key words:

Glutamate-glutamine cycle, glycolysis, lactate, Nitric Oxide, Pentose phosphate pathway

Introduction

In the central nervous system (CNS), quiescent microglia constitutes the first line of defense (Falsig et al. 2008) that reacts to acute damage or infectious agents. In a dynamic equilibrium between the lesion progression and the environment, microglia adopts a diversity of phenotypes ranging from the pro-inflammatory M1 to the neurotrophic M2 (Luo and Chen 2012). So, in response to a diversity of signals, the microglia transition to an activated state implies migration to the lesioned area, induction of phagocytosis, massive changes in gene expression, and reorganization of the cell phenotype to directly modify neuronal survival. Thus, in the same environment activated microglia interferes the responses of supporting cells through release of a diversity of factors (Kettenmann et al. 2011).

Microglia express a broad set of genes encoding proteins that include but are not limited to cytokines, chemokines, neurotrophins, neurotoxic factors, and proteases. Depending on the intensity of damage and the time post-injury, a crosstalk with neurons and astrocytes induces adaptation of the microglia phenotype to favor debris clearance, necrosis, tissue repair or regeneration (De Yebra et al. 2006). For example, with a proper timing and mode of activation, microglia work as efficient antigen-presenting cells that stimulate T cells and affect the milieu balance between neurotrophism and cytotoxicity.

Reactive microglia mediate this diversity of processes in coordination with reactive astrocytes, and both cell types depend on glucose metabolism for feeding their activities. After glucose uptake, Hexokinase (HK; E.C. 2.7.1.1) mediates glucose phosphorylation, yielding glucose-6-phosphate (G6P), a

common precursor of glycolysis for energy and lactate production, and of the pentose-phosphate pathway (PPP). In microglia, the PPP not only renders ribose-5-phosphate for nucleic acid synthesis, but also NADPH+H⁺ redox equivalents through its oxidative branch, to be transformed at the external cytoplasm membrane by NADPH oxidase (E.C. 1.6.3.1) in superoxide ions for defense and oxidative stress (Wu et al. 2006; Yang et al. 2007). The rate-limiting step in glycolysis activity is catalyzed by 6-phosphofructokinase (PFK1; E.C. 2.7.1.11), and in PPP activity by glucose-6-phosphate dehydrogenase (G6PD; E.C. 1.1.1.49). The interconnected reactions between these two pathways facilitate a direct and rapid metabolic modulation that covers at each moment the cell demand in these diverse end products.

Presently, the adaptation of glucose pathways to feed microglia diversity of phenotypes remains unknown, and we hypothesized that it might in part mimic the adaptation described in astrocytes. In astrocytes, nitric oxide (NO) formation triggers a very rapid PFK1 activation that potentiates anaerobic glycolysis versus the oxidative phosphorylation (OXPHOS). This metabolic transition preserves astrocytes from ATP depletion and maintains their mitochondrial membrane potential (Almeida et al. 2004b).

To this end, *in vitro* metabolic studies were performed in BV-2 microglia, a suitable alternative model of primary culture (Henn et al. 2009), before and after activation with LPS+ IFN γ , and NO production measured in each condition (Blasi et al. 1990). Here we provide evidences that, associated with NO formation, activation of microglia triggers a metabolic reprogramming based on an increased glucose uptake and a potentiation of both the anaerobic glycolysis and the oxidative branch of PPP, while retaining a mitochondrial activity.

Essential to ensure the new functions of activated microglia, ribose-5-phosphate availability for nucleic acid synthesis and gene transcription increases rapidly as well as ATP, lactate and NADPH+H⁺. In Discussion the role of microglia lactate formation and glutamate uptake is considered positioned within the neuroenergetics of the astrocyte-neuron lactate shuttle (ANLS) (Bouzier-Sore et al. 2003; Magistretti 2006; Magistretti and Chatton 2005; Pellerin and Magistretti 2012) of a four-partite synapse, in which lactate is shuttling to neurons not only from astrocytes but also from microglia (Rodríguez MJ 2013).

Materials and methods

Materials

Cell line of murine BV-2 microglia was purchased from Cell Bank (Interlab Cell Line Collection, ICLC, Geneva, Italy). RPMI medium supplemented with L-glutamine was purchased from GIBCO (Oklahoma, USA). Fetal Bovine Serum (FBS), was from VWR Scientific (San Francisco, USA). Culture plates and flasks were purchased from Nunc (Roskilde, Denmark). Lipopolysaccharide (LPS) from *Escherichia coli* 0111:B4 and interferon-gamma (IFN γ) and all metabolites and enzyme reagents were purchased from Sigma (St. Louis, USA).

BV-2 cell culture

BV-2 cells were cultured in RPMI 1640 medium with L-glutamine and supplemented with 10% (v/v) heat-inactivated FBS, 100 U/ml penicillin and 100

µg/ml streptomycin. Cells were grown in a humidifier cell incubator containing 5% CO₂ at 37 °C. Before activation, cells were cultured at a density of 5 × 10⁴ cells/ml for 24 h and flasks were divided into 3 groups: a) One group with no further manipulation, called Control, b) the LPS+ IFN γ group, in which BV-2 cells were activated with LPS+ IFN γ (0.1 µg/ml and 0.5 ng/ml respectively) for 24 hours, and c) the IL-4 group, in which BV-2 cells were stimulated with IL-4 (0.5 µg/ml) for 24 hours.

Inhibition of NO synthesis in LPS+IFN γ stimulated BV-2 cells

In order to inhibit NO formation, BV-2 cells activated with LPS+IFN γ were incubated with 2.5 mM N ω -nitro-L-arginine (NLA), a potent inhibitor of nitric oxide synthase (NOS) (Molnár and Hertelendy 1992).

Quantification of NO and TNF α production by BV-2 cells

NO production was assessed in culture supernatants by the Griess reaction, a colorimetric assay that detects nitrite (NO²⁻) as a stable reaction product of NO with molecular oxygen (Green et al., 1982). Briefly, 50 µl of each sample were incubated with 25 µl of Griess reagent A (1% sulfanilamide, 5% phosphoric acid) and 25 µl of Griess reagent B (0.1% N-1-naphthylenediamine) for 5 min. Sample optical density was measured at 540 nm with a microplate reader (Sunrise-Basic Reader, TECAN). The nitrite concentration was determined from a sodium nitrite standard curve. TNF α released in the cell culture supernatant was determined by an ELISA murine TNF α kit (PeproTech; London, UK) following the manufacturer's guidelines.

Real-time RT-PCR

Total RNA from microglial cells was isolated using the NucleoSpin® RNA/Protein kit (Qiagen Inc., Hilden, Germany) according to the manufacturer's instructions. Then 2 µg of first-strand cDNA was synthesized with random primers using the First Strand cDNA Synthesis kit. The RT reaction was performed at 42°C for 60 minutes and then at 70°C for 5 minutes. Real-time PCR was conducted using SensiFAST® SYBR No-ROX One-Step mix and Applied Biosystems (Foster, CA) Stem One Plus® Real Time PCR Systems according to manufacturer's instructions. The PCR program was: 2 minutes at 95°C for denaturation, subsequently 45 cycles of 15 seconds at 95°C for amplification, and 1 minute at 60°C for final extension.. The level of mRNA expression was determined with a standard curve and normalized to the mRNA level of B2m. The PCR primer of B2m endogenous control, glucose transporters (GLUT) -1, -2 -3, -4, and -5, and glucokinase (GK) target genes were purchased from RealTimePrimers (Elkins Park PA, USA) The $\Delta\Delta C_T$ method was used to analyze the data as described by Bookout et al. (2006). Primer sequences for target gene and endogenous controls are presented in Table 1.

Glucose consumption and Lactate production

Culture medium was collected from control and LPS+IFN γ activated BV-2 cells at time 0 and 24 hours. Then glucose and lactate levels were determined with an ADVIA® 2400 Clinical Chemistry System (Siemens Healthcare Diagnostics, Tarrytown, USA) that uses the glucose oxidase method described by Barham and Trinder (Barham and Trinder 1972) and the method of Shimojo (Shimojo et

al. 1989) for lactate measurement. For statistical analysis of lactate release, a normal distribution of data was assumed (Voisin et al. 2010).

Lysate preparation and enzyme activity determination

Cells were grown to confluence, transferred to a 15 ml Falcom® tube (BD Biosciences, California, USA), centrifuged at 1000x g at RT for 10 min. Pelleted cells were washed in 10 ml PBS 10 mM PH=7.4, counted in a Neubauer counting chamber and centrifuged again. The pellet was suspended in enough amount of ice-cold lysis buffer (50 mM Tris-HCl, 4 mM EDTA, 50 mM FK, 0,1% (v/v) Triton X-100, PH=7) to have 10^7 cells/ml, transferred to a 1.5 ml centrifuge tube and homogenized (Potter's Homogeneizer) at 11000 min^{-1} . Then, the cell lysate was centrifuged at 14000 g for 15 min at 4°C. The supernatant fraction was transferred to a centrifuge tube and stored at 4°C until the enzymatic assay was performed.

The enzyme activities of HK, PFK1, G6PDH and lactate dehydrogenase (LDH; E.C. 1.1.1.27) were estimated spectrophotometrically in BV-2 lysate supernatants. The assays were performed at 30°C in 1 ml final volume incubation buffer added with 100 µl cell supernatant in a Beckman Coulter (Brea, USA) recording spectrophotometer. Then concentration of NADH or NADPH was monitored by measuring absorbance at 340 nm. One unit of enzyme activity (U) is defined as µmol/min, and specific activity is expressed as U/n°cells.

HK activity was assayed by measuring the rate of reduction of NADP^+ by

glucose 6-phosphate dehydrogenase (Bergmeyer 1983). The assay medium contained Tris-HCl 50 mM, MgSO₄ 80 mM, EDTA 20 mM, KCl 1.5 mM, mercaptoethanol 2mM, NADP⁺ 3 mM, ATP 2.5 mM, Triethanolamine 200 mM, Glucose 1 mM.

PFK1 activity was measured by measuring changes in the absorbance of NADH in a coupled enzyme assay (Beutler 1975). The assay buffer consisted of Tris-HCl 50 mM, pH 7.4, MgCl₂ 100 mM, EDTA 5 mM, aldolase (mouse muscle, 0.04 U/ml), triose phosphate isomerase (mouse muscle, 2.4 U/ml), GAPDH (mouse muscle, 0.32 UI/ml) and 1mM of fructose 6-phosphate and ATP.

Lactate dehydrogenase activity was measured using the method previously described by Hakala (Hakala et al. 1956). The assay buffer consisted of Tris-HCl 50mM PH=7.5, NADH 2 mM and pyruvate 20mM.

G6PDH activity was assayed as described by Bishop (Bishop 1966). The assay medium contained 380 mM glycine, 304 mM hydrazine, 83 mM Lactate and 2,6 mM NAD disodium salt.

Confocal imaging of mitochondrial membrane potential

Mitochondrial membrane potential ($\Delta\Psi_m$) was measured by confocal imaging of BV-2 cells loaded with the fluorescent probe tetramethylrhodamine ethyl ester (TMRE) (Molecular Probes, Eugene Oregon), as previously described (Baczkó et al. 2004). In brief, cells were first incubated in 6 well-plates for 30 min in medium containing TMRE (50 nM) and then washed with fresh medium.

Afterwards, cells were incubated in the presence of 50 nM TMRE during the imaging process. Cell fluorescence was acquired by sequential scanning at the 510 nm emission wavelength. Cell average pixel intensity was obtained as an average of measurements done in 4 fields of each one of 3 culture wells.

Confocal images were obtained using Zeiss Observer.Z1® microscope coupled to a Retiga EXi Fast 1394® camera, objective LD 20X/0.4 DICII (resolution 0.83 μm).

Software and Data analysis

Statistical studies and graphics were performed with Statgraphics® (STSC Inc., Rockville, USA) and Graphpad Prism® (GraphPad Software Inc., La Jolla, USA). For each parameter, Kurtosis and Skewness moments were calculated to test the normal distribution of data. One-way ANOVA test was used to analyse differences between the groups. In all cases $p < 0.05$ was considered statistically significant.

Image acquisition was performed using Fluo4® software (Exploranova, Bordeaux, France). Figure 5 was produced using Servier Medical Art archive (Les laboratoires servier, Suresnes, France)

Results

BV-2 cell activation increases glucose uptake and its phosphorylation

BV-2 cell activation was monitored by estimation of NO and TNF α release 24h

after activation with LPS+IFN γ . At this time, LPS+IFN γ increased 6 fold NO production (from 4.89 ± 0.85 to 29.62 ± 1.96 $p < 0.0001$) and TNF α 3.5-fold (from 534.88 ± 113.94 to 1948.58 ± 333.32 $p < 0.0001$) when compared with controls.

BV-2 glucose consumption was compared between control and LPS+IFN γ activated cells. In both situations, glucose was measured in the culture medium at time 0 and 24h, and results were referred to the BV-2 cell number. After activation, glucose consumption increased significantly in a fold change of 1.37 (Figure 1A, 2D).

An increased energy demand requires greater microglia usage of glucose, and in other cells this is facilitated by the increased activity of Hexokinase to retain glucose within the cell, and also by the increased expression of GLUT. To estimate the effect of cell activation on the glucose uptake and consumption by microglia we determined the HK specific activity and the expression of GK and the five main species of GLUT. Relative to control, LPS+IFN γ promoted a significant 1.9-fold increase of HK specific activity in the soluble fraction of cell lysate (Figure 1B, 2D). BV-2 glucokinase expression was analyzed by RT-qPCR. mRNA of this enzyme was amplified from total RNA isolated from control BV-2 cells, and no change was found after LPS+IFN γ activation (data not shown).

To identify which of the five members of the GLUT family are expressed in microglia, mRNA of GLUT-1 to -5 was analyzed in control cells by RT-qPCR. GLUT-1 expression resulted largely predominant (91% of total), far from GLUT-

4 the second in abundance (8,2% of total) (Figure 1C). The very low expression of GLUT-2, GLUT-3 and GLUT-5 (< 0,2% of total) was considered negligible (Figure 1C). 24h after LPS+IFN γ activation, both GLUT-1 and GLUT-4 expression resulted similarly increased, but this increase was significant for GLUT-4 ($p=0.034$) and not for GLUT1 ($p=0,057$). GLUT-2, GLUT-3 and GLUT-5 levels remained negligible (Figure 1C).

BV-2 cell activation induces a switch of glucose metabolism to anaerobic glycolysis and pentose phosphate pathway.

The increased glucose uptake and its phosphorylation measured in activated BV-2 cells may indicate an enhancement of anaerobic glycolysis, supported by the increased activity of PFK1, the key regulatory enzyme of the glycolytic rate. This enhancement is sometimes associated with an increased ROS production at the plasma membrane facilitated by the increased activity of G6PDH, the regulatory enzyme of the PPP.

Consistent with this possibility, G6PDH specific activity was determined in the soluble fraction of cell lysate, together with PFK1 and LDH specific activities and lactate extracellular concentration. Relative to control, LPS+IFN γ activation promoted at 24h a significant increase of G6PDH specific activity in a 1.95 fold change ($p=0.004$, Figure 2A,D). PFK1 specific activity resulted also significantly increased in a 1.14 fold change ($p=0.0014$, Figure 2B,D), and the same occurred with LDH activity, increased in a fold change of 1.4 ($p<0.0001$, Figure 2C,D).

Compared to control, lactate production was doubled in the activated cells, as evidenced at 24h by its 2.02-fold increased concentration in the culture medium ($p=0.019$). Besides the increased glucose uptake of the activated cells, the lactate level represents an increased and massive transformation of G6P into lactate, supported by a glucose/lactate ratio from 1.266 in controls to 1.874 in activated cells.

This massive lactate production could be attributed to a reduced mitochondrial activity and a switch to anaerobic glycolysis of the activated cells. This was assessed through a time-lapse confocal imaging of the inner membrane potential ($\Delta\Psi_m$) at 24h in control and activated cells with the mitochondrial membrane potential sensitive dye TMRE (3A). In both situations, the frequency distribution of mitochondria fluorescence followed a normal distribution and was similar in their absolute value and relative frequency distribution (Figure 3B). The lack of $\Delta\Psi_m$ difference herein found indicates that the activated cells maintain their electron transport chain usage besides their anaerobic glycolysis switch and their increased PPP.

NO formation participates of the activated BV-2 cells glycolytic activation

Involvement of NO in the metabolic reprogramming of LPS+IFN γ activated BV-2 cells was studied after 2'5 mM N ω -nitro-l-arginine inhibition of iNOS for 24h. Glucose and lactate were measured in the culture medium at time 0 and 24h, and results referred to the BV-2 cell number. iNOS inhibition resulted in a decreased of both glucose consumption (fold change of 0.82, $p=0.02$) and lactate release (fold change of 0.63, $p<0.001$) (Figure 4A, B), back to control

values. No significant change in G6PDH was found (Figure 4C), indicating that its activation is independent from NO.

BV-2 cells adoption of a phagocytic phenotype activates a new metabolic reprogramming

To determine whether our results also apply to the adoption of a phagocytic phenotype, BV-2 cells were stimulated with IL-4 (0.5 $\mu\text{g/ml}$) for 24h. Glucose and Lactate were both measured in the culture medium at time 0 and 24h, and G6PDH activity in the homogenate as usually. With regard to control, glucose consumption was 30% reduced ($p < 0.001$) and lactate production 43% ($p < 0.006$), whereas G6PDH activity resulted unchanged. In these conditions, the maintenance of the PPP ensures NADPH+H⁺ redox equivalents to be transformed in superoxide ions for phagocytosis as G6DPH strongly increases its activity with higher NADP⁺ level. The new biomolecules delivered by phagocytosis directly available to the BV-2 cells would reduce at least in part the need of anabolic reactions and thus the cell energy demand. This possibility requires further experiments to be validated.

Discussion

BV- 2 cells were used to investigate the microglia adaptation to an excitotoxic phenotype. This cell line is considered a suitable alternative model of primary culture or of many animal studies (Henn et al. 2009) (Stansley et al. 2012). For example, 90% of the genes induced in BV-2 by LPS activation are also found in primary microglia, including the Nitric Oxide synthase (iNOS) gene. 24h after

incubation with LPS+IFN γ , BV-2 cells increased NO and TNF α production that is related with an enhancement of cell inflammatory activity (Ortega et al. 2013). In these conditions, the main finding of this study is the coordinated response of the glucose pathways necessary to cover the cell demand and enable the microglia response to activation. This metabolic reprogramming is different with microglia adoption of a phagocytic phenotype as the delivery of new biomolecules may reduce the cell energy demand. In astrocytes LPS stimulation induced NO production leading to an increased glucose consumption and lactate release (Bolaños et al. 1994) and an increased PPP activity to prevent glutathione depletion and increase astrocyte resistance to NO mediated cellular damage (García-Nogales et al. 1999). After exposure to peroxynitrite, the maintenance of astrocyte mitochondrial activity and its reduction in neurons also demonstrates the astrocytic resistance capacity to NO damage (Bolaños et al. 1995). The direct NO participation in the microglia metabolic reprogramming shown by our data reinforces the similarity with the astrocyte metabolic adaptation to excitotoxicity. As such, the increased HK activity and increased GLUT1 and GLUT4 expression ensure enough glucose availability to the cell. GLUT1 expression in control microglia was much higher than GLUT4, with similar changes 24h after activation. Because of that, these two transporters can be considered constitutive of microglia.

GLUT1 is a high-affinity glucose transporter, which expression in tumor cells is stimulated under hypoxic conditions. And this adaptation also includes enhancement of the glycolysis rate to support the increased energy demand of the proliferative cells (Bashan et al. 1992; Haber et al. 1998). The HK and

GLUT1 increases herein found would then reflect the microglia adaptation to an enhanced glycolytic demand with a high lactate production, and high metabolic rate. GLUT4 expression is modulated in brain and pancreas by ATP dependent potassium (K_{ATP}) channels whose activity depends on glucokinase (Choeiri et al. 2006). In agreement with previous brain studies (Alvarez et al. 2002) the low glucokinase K_m that renders the enzyme unable to detect glucose concentration increase may explain the unchanged glucokinase expression in activated microglia. The increased K_{ATP} channel expression described in activated microglia (Ortega et al. 2012; Ramonet et al. 2004b) may then participate in the GLUT4 expression increase. If true, the similar changes of GLUT1 and GLUT4 shown by our results suggest a coordinated microglia control of their expression that may depend, at least in part, on K_{ATP} channel activity. As observed in taste cells (Yee et al. 2011), this would represent a fine coordination between activation of microglia and increased glucose availability.

Microglia metabolic reprogramming led to a potentiation of anaerobic glycolysis reflected by the increased PFK1 and LDH activities and a massive lactate formation. In astrocytes increased NO stimulates PFK1 activity through allosteric activation with fructose-2,6-bisphosphate (Fru-2,6-P₂) produced by 6-phosphofructo-2-kinase/fructose-2,6-bisphosphatase. Moreover, NO inhibition of cytochrome c oxidase switches the glycolytic rate on, with pyruvate conversion into lactate recovering NAD⁺ in the cytosol for glycolysis feed-back (Almeida et al. 2004a). The supply of glucose-derived lactate by activated microglia would support active neurons, whose elevated energy demand relies mostly on mitochondrial ATP production. Thus, with the astrocytes and

microglia adapted to a major glucose anaerobic oxidation, lactate represents the major neuronal energy source in damaged CNS (Fig 5).

The NO-mediated down-regulation of mitochondrial energy production observed in neurons and initially in astrocytes (Bolaños et al. 1994), but afterwards considered to be unaffected by the same authors, with similar activities of the enzymatic complexes of the Krebs cycle (Bolaños et al. 1995) was not truly observed in microglia. The similar $\Delta\Psi_m$ of control and activated BV-2 cells might reflect the ATP synthase reversed reaction fed by ATP from glycolysis and others (Almeida et al. 2001 PNAS), or could indicate an active electron transport chain energy production. In microglia of damaged brain tissue, the higher number of mitochondria labeled with [H^3]PK11195 (Bernal et al. 2009; De Yebra et al. 2006) and their higher K_{ATP} channels expression (Rodríguez MJ 2013; Virgili et al. 2011) argue in favor of a significant mitochondrial production of energy to help ensuring sufficient bioenergetics to execute the new transcription programs derived from excitotoxic activation. If true, feeding of the Krebs cycle to maintain mitochondria activity cannot rely on pyruvate because of its transformation into lactate, but on 2-oxoglutarate formation from glutamate and glutamine deamination that increases progressively from apoptotic to necrotic damage (Ramonet et al. 2004a).

Upon activation, microglia express the two glutamate transporters EAAT-1 and -2 for glutamate and glutamine synaptic extrusion as well as glutamine synthase (Gras et al. 2006). Thus, in excitotoxicity, the fast microglial uptake of glutamate and glutamine, coordinated with the astrocyte glutamate removal, promotes a quick deactivation of the increased synaptic glutamate signal. In astrocytes, the

early work by Pellerin et al (1994) describes the glutamate-induced glycolysis to facilitate lactate to neurons during physiological activation, and hypothesized for the first time the ANLS. With excitotoxicity, microglia glutamate uptake would induce a similar stimulatory effect to provide further lactate to neurons, and also renders abundant 2-oxoglutarate to ensure the Krebs cycle activity.

In microglia glutamate deamination renders 2-oxoglutarate and ammonium that, combined with CO₂ released from the Krebs cycle, forms carbamic acid, a precursor of the pyrimidine bases necessary for nucleic acid synthesis and the increased gene expression. As in astrocytes (Gradinaru et al. 2012), carbamic acid direct clearance and elimination as a stable complex with glucuronides is also possible through a detoxification process (Hipkiss 2010; Schafer et al. 2013).

In necrotic brain tissue a net glutamine output of the Glutamate/Glutamine cycle caused by a reduced neuronal glutaminase activity (Ramonet et al. 2004a) increases the microglial formation of 2-oxoglutarate and ammonium and the generation of superoxide ions. After reaction with NO, superoxide ions form the highly reactive peroxynitrite products, associated with a cytotoxic microglia phenotype, and a progressive microglia dysfunction. (Svoboda and Kerschbaum 2009). If true, microglia ammonium concentration would represent one of the contextual factors that influence the microglial net effects on neuronal survival (Luo and Chen 2012) (See Fig. 5).

The PPP oxidative branch was also increased in activated microglia, as shown by the increased G6PDH activity that supports G6P oxidation and NADPH formation. In neurons NO facilitates a fine-tuning of G6P destination to glycolysis or PPP that potentiates glutathione reduction against oxidative

damage. Our data indicate that NO is also directly involved in the metabolic reprogramming of microglia, together with a significant contribution of the phagosomal NADPH-oxidase to ROS generation and oxidative stress damage from G6P (Miller et al. 2007; Wu et al. 2006). Furthermore, the juxtaposition of phagosomes and mitochondria recently proposed in microglia (Rodríguez MJ 2013) should potentiate mitochondrial ROS formation and energy production (Dikalov et al. 2012; Murphy 2009) (See Fig. 5).

In conclusion, NO appears to play a key role in the adaptation of activated microglia to the energy commitment necessary to ensure its adoption of a neurotrophic/cytotoxic phenotype. In these conditions, the coordinated response of the four-partite synapse, in which lactate is shuttling to neurons not only from astrocytes but also from microglia, has also to include the rapid glutamate removal by astrocytes and microglia. Thus, under brain damage, a new player should be included in the ANLS initially proposed by Pelerin et al. (1994), transforming it into a microglia-astrocyte-neuron lactate shuttle. Further studies are needed to determine how reduction of glutaminase activity following neuronal damage and the consequent increased ammonium output influence the microglia response of increased oxidative damage.

Acknowledgements

We thank Ivan Cester and Dra. Martínez-Moreno for technical help and Laura Gómez for performing the G6PDH activity determinations. Authors disclose any potential sources of conflict of interest.

References

- Almeida A, Moncada S, Bolaños JP. 2004a. Nitric oxide switches on glycolysis through the AMP protein kinase and 6-phosphofructo-2-kinase pathway. *NatCell Biol* 6(1):45-51.
- Almeida A, Moncada S, Bolaños JP. 2004b. Nitric oxide switches on glycolysis through the AMP protein kinase and 6-phosphofructo-2-kinase pathway. *Nat Cell Biol* 6(1):45-51.
- Alvarez E, Roncero I, Chowen JA, Vázquez P, Blázquez E. 2002. Evidence that glucokinase regulatory protein is expressed and interacts with glucokinase in rat brain. *J Neurochem* 80:45-53.
- Baczkó I, Giles WR, Light PE. 2004. Pharmacological activation of plasma-membrane KATP channels reduces reoxygenation-induced Ca(2+) overload in cardiac myocytes via modulation of the diastolic membrane potential. *British Journal of Pharmacology* 141(6):1059-1067.
- Barham D, Trinder P. 1972. An improved colour reagent for the determination of blood glucose by the oxidase system. *Analyst* 97(151):142-145.
- Bashan N, Burdett E, Hundal HS, Klip A. 1992. Regulation of glucose transport and GLUT1 glucose transporter expression by O₂ in muscle cells in culture. *Am J Physiol* 262(3 Pt 1):C682-690.
- Bergmeyer HU, Grassl, M., and Walter, H.E. 1983. *Methods of Enzymatic Analysis*. Deerfield Beach, FL: Bergmeyer, H.U.
- Bernal F, Petegnief V, Rodríguez MJ, Ursu G, Pugliese M, Mahy N. 2009. Nimodipine inhibits TMB-8 potentiation of AMPA-induced hippocampal neurodegeneration. *J Neurosci Res*. p 1240-1249.
- Beutler E. 1975. *Red Cell Metabolism. A Manual of Biochemical Methods*. Biochemical Methods (ed 2) Orlando, Fla, Grune & Stratton 2 Edition.
- Bishop C. 1966. Assay of glucose-6-phosphate dehydrogenase (E.C. 1.1.1.49) and 6-phosphogluconate dehydrogenase (E.C. 1.1.1.43) in red cells. *J Lab Clin Med* 68(1):149-155.

- Blasi E, Barluzzi R, Bocchini V, Mazzolla R, Bistoni F. 1990. Immortalization of murine microglial cells by a v-raf/v-myc carrying retrovirus. *J Neuroimmunol* 27(2-3):229-237.
- Bolaños JP, Heales SJ, Land JM, Clark JB. 1995. Effect of peroxynitrite on the mitochondrial respiratory chain: differential susceptibility of neurones and astrocytes in primary culture. *J Neurochem* 64(5):1965-1972.
- Bolaños JP, Peuchen S, Heales SJ, Land JM, Clark JB. 1994. Nitric oxide-mediated inhibition of the mitochondrial respiratory chain in cultured astrocytes. *J Neurochem* 63(3):910-916.
- Bouzier-Sore A-K, Voisin P, Canioni P, Magistretti PJ, Pellerin L. 2003. Lactate Is a Preferential Oxidative Energy Substrate Over Glucose for Neurons in Culture. *J Cereb Blood Flow Metab*:1298-1306.
- Choeiri C, Staines WA, Miki T, Seino S, Renaud J-M, Teutenberg K, Messier C. 2006. Cerebral glucose transporters expression and spatial learning in the K-ATP Kir6.2(-/-) knockout mice. *Behav Brain Res* 172(2):233-239.
- De Yebra L, Malpesa Y, Ursu G, Pugliese M, LiÇvens JC, Kerkerian-Le Goff L, Mahy N. 2006. Dissociation between hippocampal neuronal loss, astroglial and microglial reactivity after pharmacologically induced reverse glutamate transport. *Neurochemistry International* 49 (7):691-697.
- Dikalov SI, Li W, Doughan AK, Blanco RR, Zafari AM. 2012. Mitochondrial reactive oxygen species and calcium uptake regulate activation of phagocytic NADPH oxidase. *Am J Physiol Regul Integr Comp Physiol* 302(10):R1134-1142.
- Falsig J, van Beek J, Hermann C, Leist M. 2008. Molecular basis for detection of invading pathogens in the brain. *J Neurosci Res* 86(7):1434-1447.
- García-Nogales P, Almeida A, Fernández E, Medina JM, Bolaños JP. 1999. Induction of glucose-6-phosphate dehydrogenase by lipopolysaccharide contributes to preventing nitric oxide-mediated glutathione depletion in cultured rat astrocytes. *J Neurochem* 72(4):1750-1758.
- Gradinaru D, Minn A-L, Artur Y, Minn A, Heydel J-M. 2012. Effect of oxidative stress on UDP-glucuronosyltransferases in rat astrocytes. *Toxicol Lett* 213(3):316-324.

- Gras G, Porcheray F, Samah B, Leone C. 2006. The glutamate-glutamine cycle as an inducible, protective face of macrophage activation. *J Leukoc Biol* 80(5):1067-1075.
- Haber RS, Rathan A, Weiser KR, Pritsker A, Itzkowitz SH, Bodian C, Slater G, Weiss A, Burstein DE. 1998. GLUT1 glucose transporter expression in colorectal carcinoma: a marker for poor prognosis. *Cancer* 83(1):34-40.
- Hakala M, Glaid AJ, Schwert GW. 1956. Lactic dehydrogenase. II. Variation of kinetic and equilibrium constants with temperature. *J Biol Chem* 221(1):191-209.
- Henn A, Lund S, Hedtjärn M, Schratzenholz A, Pörzgen P, Leist M. 2009. The suitability of BV2 cells as alternative model system for primary microglia cultures or for animal experiments examining brain inflammation. *ALTEX* 26(2):83-94.
- Hipkiss AR. 2010. Aging, Proteotoxicity, Mitochondria, Glycation, NAD and Carnosine: Possible Inter-Relationships and Resolution of the Oxygen Paradox. *Front Aging Neurosci* 2:10.
- Kettenmann H, Hanisch U-K, Noda M, Verkhratsky A. 2011. Physiology of microglia. *Physiol Rev* 91(2):461-553.
- Luo X-G, Chen S-D. 2012. The changing phenotype of microglia from homeostasis to disease. *Transl Neurodegener* 1(1):9.
- Magistretti PJ. 2006. Neuron-glia metabolic coupling and plasticity. *J Exp Biol* 209(Pt 12):2304-2311.
- Magistretti PJ, Chatton J-Y. 2005. Relationship between L-glutamate-regulated intracellular Na⁺ dynamics and ATP hydrolysis in astrocytes. *J Neural Transm* 112(1):77-85.
- Miller RL, Sun GY, Sun AY. 2007. Cytotoxicity of paraquat in microglial cells: Involvement of PKCdelta- and ERK1/2-dependent NADPH oxidase. *Brain Research* 1167:129-139.
- Molnár M, Hertelendy F. 1992. N omega-nitro-L-arginine, an inhibitor of nitric oxide synthesis, increases blood pressure in rats and reverses the pregnancy-induced refractoriness to vasopressor agents. *Am J Obstet Gynecol* 166(5):1560-1567.
- Murphy MP. 2009. How mitochondria produce reactive oxygen species. *Biochem J* 417(1):1-13.

- Ortega FJ, Jolkkonen J, Mahy N, Rodríguez MJ. 2013. Glibenclamide enhances neurogenesis and improves long-term functional recovery after transient focal cerebral ischemia. *J Cereb Blood Flow Metab* 33:8.
- Pellerin L, Magistretti PJ. 2012. Sweet sixteen for ANLS. *J Cereb Blood Flow Metab* 32(7):1152-1166.
- Ramonet D, Rodriguez MJ, Fredriksson K, Bernal F, Mahy N. 2004a. In vivo neuroprotective adaptation of the glutamate/glutamine cycle to neuronal death. *Hippocampus* 14(5):586-594.
- Ramonet D, Rodriguez MJ, Pugliese M, Mahy N. 2004b. Putative glucosensing property in rat and human activated microglia. *Neurobiology of Disease* 17:1-9.
- Rodríguez MJ M-M, M, Ortega FJ, and Mahy N. 2013. Targeting microglial KATP channels to treat neurodegenerative diseases: a mitochondrial issue. *J Oxid Med Cell Long* (In press).
- Schafer DP, Lehrman EK, Stevens B. 2013. The "quad-partite" synapse: Microglia-synapse interactions in the developing and mature CNS. *Glia* 61(1):24-36.
- Shimojo N, Naka K, Nakajima C, Yoshikawa C, Okuda K, Okada K. 1989. Test-strip method for measuring lactate in whole blood. *Clin Chem* 35(9):1992-1994.
- Stansley B, Post J, Hensley K. 2012. A comparative review of cell culture systems for the study of microglial biology in Alzheimer's disease. *J Neuroinflammation* 9:115.
- Svoboda N, Kerschbaum HH. 2009. L-Glutamine-induced apoptosis in microglia is mediated by mitochondrial dysfunction. *Eur J Neurosci* 30(2):196-206.
- Virgili N, Espinosa-Parrilla JF, Mancera P, Pastén-Zamorano A, Gimeno-Bayon J, Rodríguez MJ, Mahy N, Pugliese M. 2011. Oral administration of the KATP channel opener diazoxide ameliorates disease progression in a murine model of multiple sclerosis. *J Neuroinflammation* 8:149.
- Voisin P, Bouchaud V, Merle M, Diolez P, Duffy L, Flint K, Franconi J-M, Bouzier-Sore A-K. 2010. Microglia in Close Vicinity of Glioma Cells: Correlation Between Phenotype and Metabolic Alterations. *Front Neuroenerg* 2:1-15.

- Wu D-C, Ré DB, Nagai M, Ischiropoulos H, Przedborski S. 2006. The inflammatory NADPH oxidase enzyme modulates motor neuron degeneration in amyotrophic lateral sclerosis mice. *Proc Natl Acad Sci USA* 103(32):12132-12137.
- Yang D, Elnér SG, Bian Z-M, Till GO, Petty HR, Elnér VM. 2007. Pro-inflammatory cytokines increase reactive oxygen species through mitochondria and NADPH oxidase in cultured RPE cells. *Exp Eye Res* 85(4):462-472.
- Yee KK, Sukumaran SK, Kotha R, Gilbertson TA, Margolskee RF. 2011. Glucose transporters and ATP-gated K⁺ (KATP) metabolic sensors are present in type 1 taste receptor 3 (T1r3)-expressing taste cells. *Proc Natl Acad Sci USA* 108(13):5431-5436.

Figure legends

Figure 1: 24h after LPS+INF γ activation, the BV-2 increased glucose consumption is facilitated by the coordinated increase of hexokinase activity and GLUT-1 and GLUT-4 expression. **A:** Increase of Glucose consumption (*p<0.0001 vs control) **B:** Increase of Hexokinase specific activity (*p=0.044 vs control). (Data are normalized for cell number; Glc_i = Glucose concentration at time 0, Glc_f = Glucose concentration at time 24h). **C:** Similar increase of GLUT-1 and GLUT-4 expression measured by Quantitative PCR analysis; Ratio is measured versus a housekeeping gene (HG, beta-2-microglobulin).

Figure 2: Coordinated BV-2 cell metabolic adaptation to LPS+IFN γ activation. **A:** Glucose-6-phosphate deshydrogenase (G6PDH) specific activity normalized by number of cells (*p=0.004). **B:** Phosphofructokinase-1 (PFK) specific activity normalized by cell concentration (*p=0.0014) **C:** Lactate deshydrogenase (LDH) specific activity normalized by cell concentration (*p<0.0001 vs control). **D:** Lactate released by BV-2 cells (*p=0.019 vs control). **E:** BV-2 cell activation increases both Glucose uptake and its transformation to lactate. (Conc. in mg.dl⁻¹. 10⁶cell⁻¹, and enzyme activities in U. 10⁶cell⁻¹).

Figure 3: Mitochondrial membrane potential of activated and non activated microglial BV2 cells. Confocal image of control (**A**) and LPS+INF γ activated (**B**) BV-2 cells loaded with the mitochondrial membrane potential sensitive dye

TMRE (40x image). **C**: Frequency distribution of mitochondrial TMRE

fluorescence in control and LPS+INF activated BV-2 cells.

Figure 4: Effect of stimulation with IL-4 and inhibition of iNOS with NLA in BV-2 cells metabolism (Data are normalized for cell number). **(A)** Glucose consumption was 30% reduced by IL-4 (* $p < 0.001$ vs control) in control BV2 cells, and NLA reduced 18% glucose consumption when applied to activated cells (# $p = 0.02$, LPS+IFN+NLA vs LPS+IFN) **(B)** Lactate release was 44% reduced by IL-4 (* $p < 0.001$ vs control) and NLA reduced 38% this lactate production in activated cells (# $p = 0.001$, LPS+IFN+NLA vs LPS+IFN). **(C)** IL-4 and inhibition of iNOS with NLA did not modified G6PDH activity.

Figure 5. Proposed microglia-astrocyte-neuron lactate shuttle (MANLS).

After microglia activation with LPS+IFN, glucose is mostly oxidized by astrocytes and microglia and converted into lactate that is taken up by neurons for its complete oxidation. Glutamine and glutamate synaptic removal by microglia fuels the tricarboxylic acid cycle to maintain mitochondrial activity and ATP generation. Initially the resulting ammonium facilitates carbamic acid synthesis for pyrimidine formation and can also be cleared as carbamic acid glucuronides.

Dashed arrows: Type 1 represents glutamine and glutamate cycle. Type 2 represent glucose metabolism. Type 3 represent non direct metabolic connections. Type 4 ammonia uptake. Glc: glucose, Glu: glutamate, Gln: glutamine, Pyr: pyruvate, Lac: lactate, G6P: glucose-6-phosphate, G3P: glucose-3-phosphate, F6P: fructose-6-phosphate, Ri5P: ribulose-5-phosphate, R5P: ribose-5-phosphate, KG: alpha ketoglutarate. NADPH: Nicotinamide adenine

dinucleotide phosphate, NTs: Nucleotides, ROS: reactive oxygen species. TCA: tricarboxylic acid cycle, CbA: carbamic acid, CbA-GC: glucuronic acid synthesis from carbamic acid. NH_4^+ : Ammonium, CO_2 : carbon dioxide

Tables

Table 1: Primer and probe sequences for real-time RT-PCR

Target	Gene	Sequence (5'-3')	Size (bp)	Accession N
Slc2a1	Mouse GLUT-1	F: TGC CAA GCT AAT CTG TAG GG	163	NM_011400
		R: GAA TGG GCG AAT CCT AAA AT		
Slc2a2	Mouse GLUT-2	F: AAG ACA AGA TCA CCG GAA CC	224	NM_031197
		R: TGG TGT TGT GTA TGC TGG TG		
Slc2a3	Mouse GLUT-3	F: TTT TCC ACA GGT CAC TGG AT	204	NM_011401
		R: GTT AGA GGA GTC GCC TTT CC		
Slc2a4	Mouse GLUT-4	F: TCC CTT TTA GAG CAG GAG GT	152	NM_009204
		R: ACA GGG AAG AGA GGG CTA AA		
Slc2a5	Mouse GLUT-5	F: GAC ACT CCC TGC TGA AGA AA	241	NM_019741
		R: CCG TAG AAG ACA CCA CAT CC		
GK	Mouse Glucokinase	F: GCC AAA AAC ACG TAT GGA AC	153	NM_008194
		R: AGC TAT AGC CAC GGA ACC TT		
B2m	Beta-2 microglobulin	F: GGC CTG TAT GCT ATC CAG AA	198	NM_009735
		R: GAA AGA CCA GTC CTT GCT GA		

FIGURE 1:

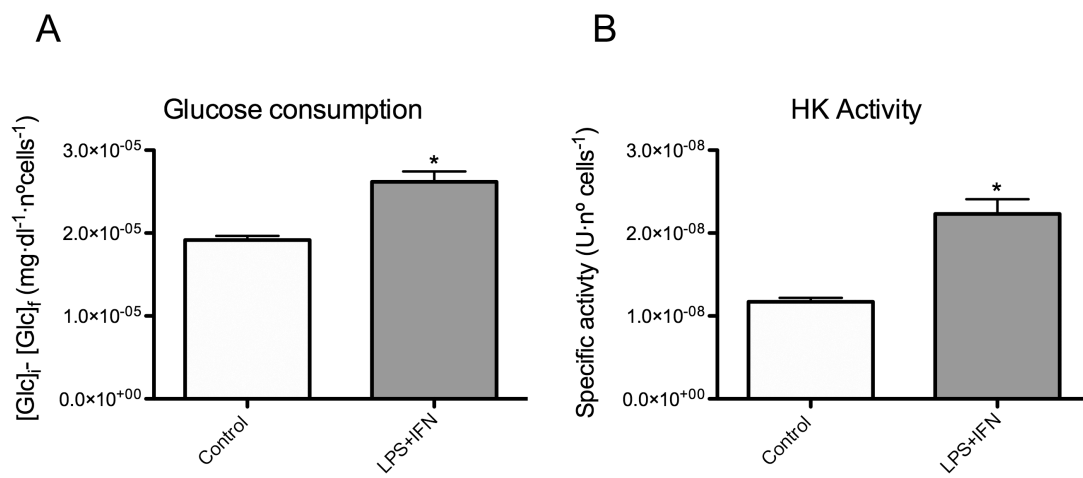


FIGURE 2:

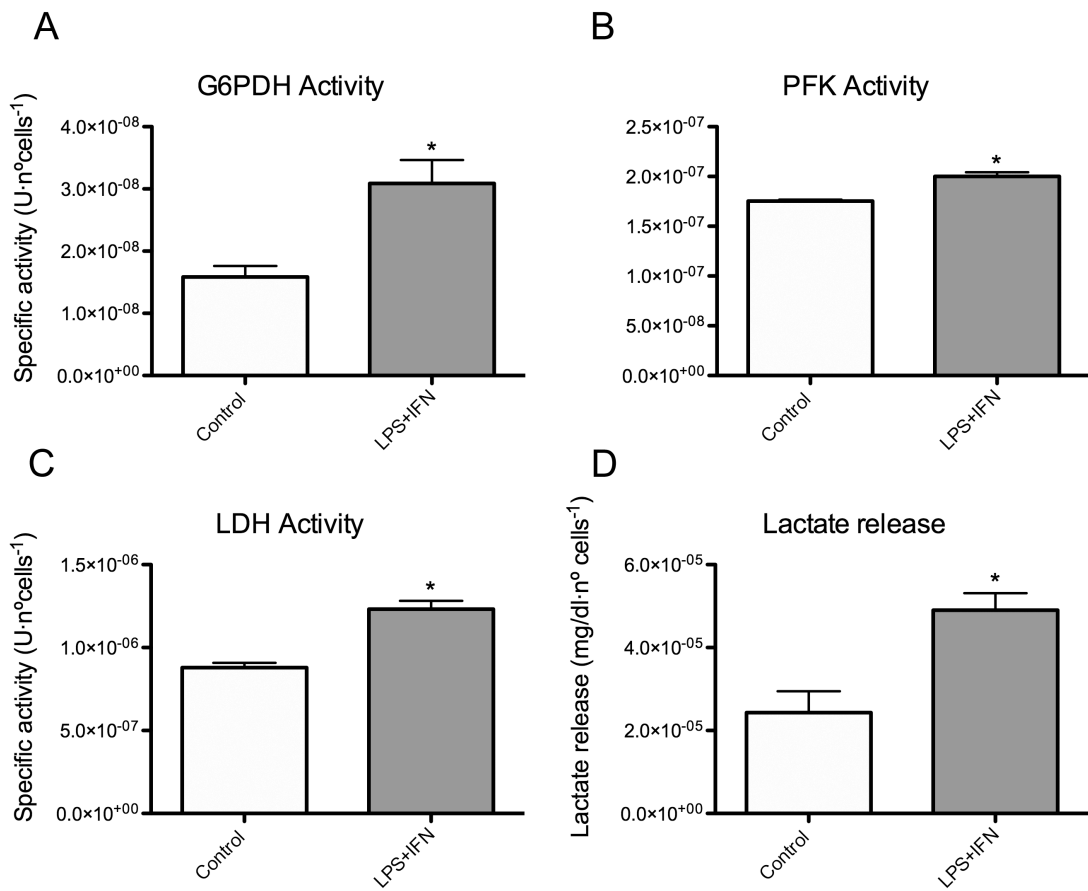


FIGURE 3:

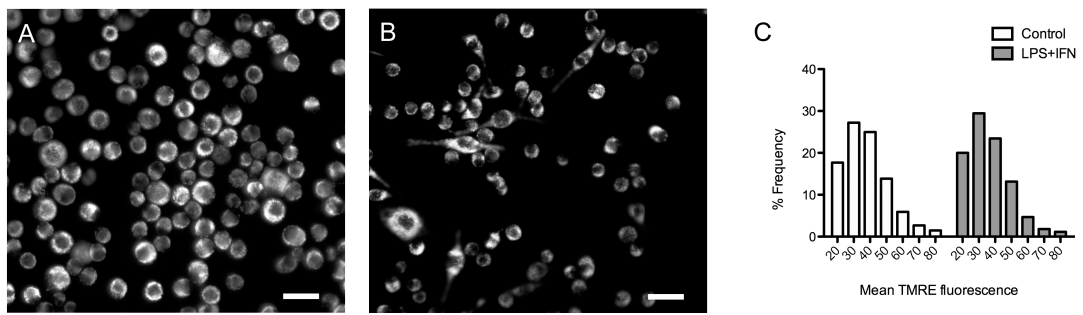


FIGURE 4:

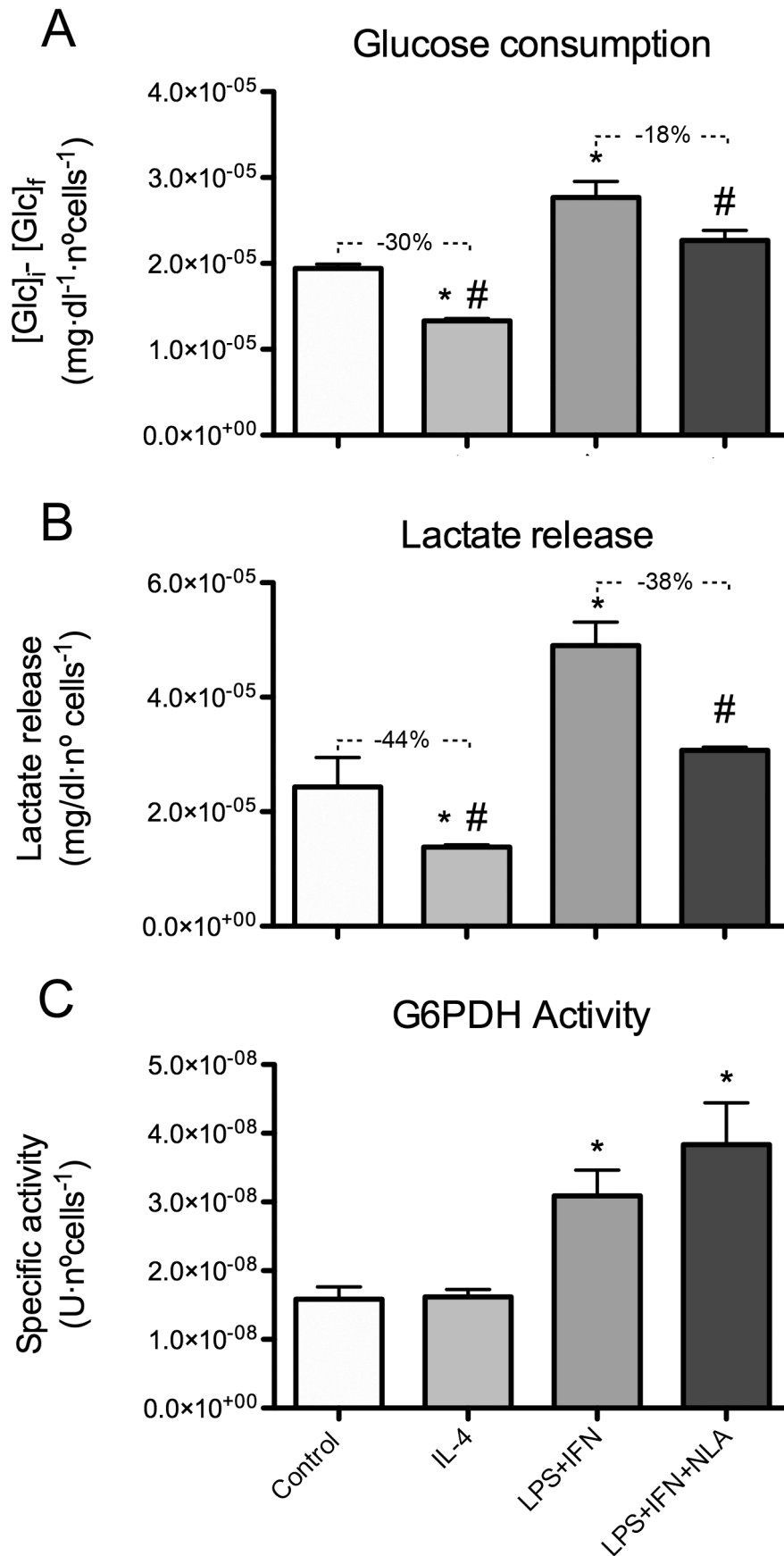


FIGURE 5:

